

arXiv:2412.15430v1 [cs.RO] 19 Dec 2024

An Environment-Adaptive Position/Force Control Based on Physical Property Estimation

TOMOYA KITAMURA^{1,2}, (Member, IEEE), YUKI SAITO², (Member, IEEE), HIROSHI ASAI², (Member, IEEE), KOUHEI OHNISHI², (Life Fellow, IEEE).

¹Department of Electrical Engineering Faculty of Science and Technology, Tokyo University of Science, Noda, Japan

²Haptics Research Center, Keio University, Kanagawa, Japan (e-mail: t.kitamura@rs.tus.ac.jp, ysaito@haptics-c.keio.ac.jp, h-asai@haptics-c.keio.ac.jp, ohnishi@sd.keio.ac.jp)

Corresponding author: Tomoya Kitamura (e-mail: t.kitamura@rs.tus.ac.jp).

The part of this work has been supported by the JST-Mirai Program Grant Number JPMJMI21B1, Japan.

ABSTRACT The technology for generating robot actions has significantly contributed to the automation and efficiency of tasks. However, the ability to adapt to objects of different shapes and hardness remains a challenge for general industrial robots. Motion reproduction systems (MRS) replicate previously acquired actions using position and force control, but generating actions for significantly different environments is difficult. Furthermore, methods based on machine learning require the acquisition of a large amount of motion data. This paper proposes a new method that matches the impedance of two pre-recorded action data with the current environmental impedance to generate highly adaptable actions. This method recalculates the command values for position and force based on the current impedance to improve reproducibility in different environments. Experiments conducted under conditions of extreme action impedance, such as position control and force control, confirmed the superiority of the proposed method over MRS. The advantages of this method include using only two sets of motion data, significantly reducing the burden of data acquisition compared to machine learning-based methods, and eliminating concerns about stability by using existing stable control systems. This study contributes to improving robots' environmental adaptability while simplifying the action generation method.

INDEX TERMS Force control, motion reproduction system, physical property estimation, position control

I. INTRODUCTION

In recent years, the importance of robotic technology has been increasingly acknowledged across various sectors, including industry, domestic applications, and healthcare [1]–[3]. For robots to operate effectively in these diverse settings, they must be capable of adapting to objects with different shapes and levels of stiffness. This adaptation often involves understanding the object's impedance, which combines force and position, making impedance adjustment a key challenge in robot control. Control operations must address both position and force dimensions to adapt seamlessly to the surrounding environment.

To simultaneously manage both position and force dimensions, various hybrid control strategies that incorporate acceleration have been proposed [4], [5]. These strategies utilize acceleration reference values generated by two distinct controllers, one dedicated to position and the other to force.

Furthermore, motion reproduction systems (MRS) have been developed to steer robotic actions using historical position and force data, aiming to replicate these actions accurately [6], [7]. Nonetheless, these approaches face challenges, especially when there is a mismatch between the environmental impedance at the time of data recording and the current environmental conditions, risking damage to the object and control instability. Progress is being made in developing MRS that adapts to environmental changes [8], [9], yet these systems often need to pay more attention to the original action's impedance [8]. In other words, if the original intention of the action was to reach a desired position, accurately reproducing both the position and force values is not the objective. Given that the environmental impedance can differ from that at the time of recording, it's impossible to accurately replicate both position and force values. What the user expects from the motor is to follow the recorded position. Therefore, infer-

ring the intention behind the recorded action and generating command values for position and force to fulfill that intention is a preferred method in motion reproduction. Additionally, there are proposals for adjusting control stiffness based on environmental feedback, but the sequential modification of control gains poses a risk to the stability of the control system [9].

Alternative approaches involving machine learning for environmental adaptation have been explored. Notably, reinforcement learning techniques have demonstrated potential in autonomously generating actions for tasks like pick-and-place or peg-in-hole operations [10]–[13]. Despite this progress, these methods are data-intensive, requiring extensive motion data for effective learning. Imitation learning, which involves capturing human movements, analyzing their characteristics, and replicating them, has also been studied [14]–[17]. However, imitation learning also requires a large amount of data, and the need for high-precision computations increases its cost.

This paper proposes a novel approach that ensures impedance matching between the environment and the motion. The method begins by recording motion data from a motor interacting with two samples of differing environment impedance. As a result, the estimation of the motion impedance becomes possible based on these two data sets. Next, the environmental impedance of a new sample is sequentially estimated through the analysis of physical property parameters. The system adjusts the motion by matching the impedance of the new sample with the approximated linear impedance curves derived from the two initial samples. The point where these two impedance lines intersect is used to determine the control command for the motion. This approach enables the generation of motions that adapt to environments with different impedance characteristics, even those that differ from the initial samples. This paper aims to enhance the adaptability of robot movements across diverse environmental conditions through the proposed impedance matching method.

In our experiments, six samples were prepared. For two samples, data was recorded during the execution of either position or force control. The proposed method was then applied to the remaining four samples. A single-degree-of-freedom rotary motor was utilized for these experiments. The effectiveness of the proposed method was assessed under extreme conditions, such as force control (i.e., zero motion impedance) and position control (i.e., infinite motion impedance). Additionally, we compared the control performance of our method with that of the MRS. The results confirmed that our proposed method significantly enhances control performance in position and force dimensions.

The primary advantage of this method lies in its ability to manage tasks of both position and force control within the same system while limiting the need for data acquisition to just two sets of motion data. Consequently, this paper makes the following contributions:

- The proposed method achieved approximately a 70%

reduction in position errors for position control tasks and force errors for force control tasks compared to traditional MRS. Generating command values and utilizing existing stable controllers ensure system stability without the need for additional stability analysis.

- By estimating the motion's impedance from two sets of data and aligning it with the environmental impedance, this approach reduces the amount of preliminary motion data required compared to machine learning-based methods and simplifies the learning process. Additionally, because it applies to environments corresponding to the extrapolation of two actions, it has a broader application scope than methods using machine learning.
- The method proposes characterizing motion skills through impedance parameters. Therefore, abstract representation of behavior opens up potential applications in teaching skills to beginners, among other possibilities.

The remainder of this paper is organized as follows. Section II focuses on the methodology, providing detailed explanations of hybrid control, MRS, physical property estimation method, and the proposed method. Section III introduces the experimental methodology, describing the experimental design and procedures using a single-degree-of-freedom rotary motor. Section IV presents the experimental results and compares the effectiveness of MRS and the proposed method. It includes a statistical verification using the t-test, providing a deep consideration of the utility of the proposed method. Finally, Section V concludes the paper, summarizing the key points of this research and discussing future research directions.

II. METHODS

A. HYBRID CONTROL

This section discusses hybrid control, which orchestrates position and force control by utilizing acceleration reference values. It begins by elucidating the concepts of position and force control and then describes how hybrid control combines these two aspects synergistically.

1) Position control

Position control is performed so the current position response value x^{res} approaches the desired position command value x^{cmd} . Therefore, the acceleration reference value in position control \ddot{x}_p^{ref} is described by (1).

$$\ddot{x}_p^{\text{ref}} = (K_{\text{pos}} + K_{\text{vel}} \frac{d}{dt})(x^{\text{cmd}} - x^{\text{res}}), \quad (1)$$

where, K_{pos} and K_{vel} represent proportional and differential gains, respectively. Furthermore, by adding the estimated disturbance \hat{f}^{dis} estimated by the disturbance observer [18], robust control against unknown disturbances is achieved.

$$\ddot{x}_p^{\text{ref}} = (K_{\text{pos}} + K_{\text{vel}} \frac{d}{dt})(x^{\text{cmd}} - x^{\text{res}}) + \hat{f}^{\text{dis}}/J_n, \quad (2)$$

where, J_n represents nominal inertia of motor.

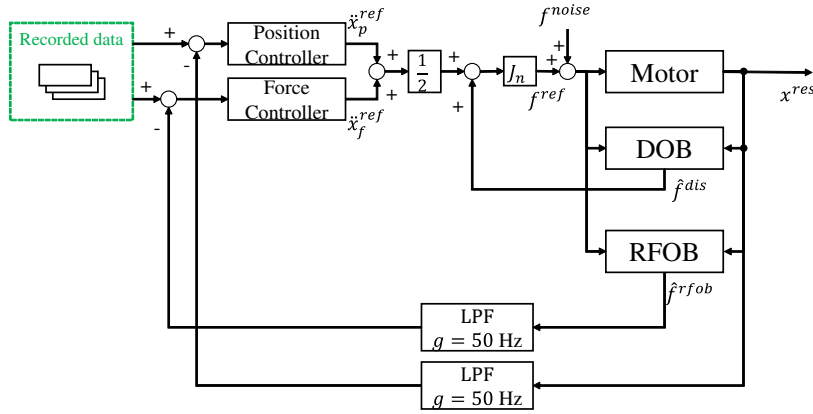


FIGURE 1: Block diagram with MRS

2) Force control

The acceleration reference value in force control \ddot{x}_f^{ref} to satisfy the desired force command value f^{cmd} is expressed by (3).

$$\ddot{x}_f^{ref} = K_{for}(f^{cmd} - \hat{f}^{rfob})/J_n + \hat{f}^{dis}/J_n, \quad (3)$$

where, K_{for} represents the force feedback gain. Additionally, the reaction force estimated by the reaction force observer [18] is denoted as \hat{f}^{rfob} .

3) Hybrid control

Hybrid control uses reference values that follow both position and force commands. Therefore, control in two dimensions is achieved by (4), which adds (2) and (3).

$$\ddot{x}^{ref} = (K_{pos} + K_{vel} \frac{d}{dt})(x^{cmd} - x^{res})/2 + K_{for}(f^{cmd} - \hat{f}^{rfob})/2J_n + \hat{f}^{dis}/J_n. \quad (4)$$

The force reference value to the motor is expressed in (5) by multiplying the moment of inertia by (4).

$$f^{ref} = J_n(K_{pos} + K_{vel} \frac{d}{dt})(x^{cmd} - x^{res})/2 + K_{for}(f^{cmd} - \hat{f}^{rfob})/2 + \hat{f}^{dis}. \quad (5)$$

From the explanation above, it becomes possible to control both the position and force command values. However, suppose the ratio of these command values, representing the motion's impedance, does not match the impedance of the actual contact environment. In that case, controlling the motor with both command values is not feasible. When there is a discrepancy between the two impedances, the controlling impedance, namely the ratio of gains between position control and force control, dictates which command value will be prioritized.

B. MRS

This section discusses the MRS, which reproduces previously acquired motions. In general, in MRS, motion data is initially obtained through bilateral control. Bilateral control

is a type of leader-follower system where the follower not only tracks the leader's position but also provides feedback to the leader about the reaction force felt by the follower, enabling bidirectional remote operation [19], [20]. By operating bidirectionally, the leader can remotely control the follower as if they were directly manipulating it. The position and force data captured in this process include the leader's movements and the adaptability to the environment involving the use of force. Since this paper does not employ bilateral control, detailed explanations of bilateral control are deferred to the references [19], [20]. This paper used the MRS to control the motor using the position and force measured during a previously executed action.

In MRS, the recorded position x^{rec} and force f^{rec} response values are the command values for control. Therefore, the force reference value is indicated by substituting the recorded response value into (5).

$$f^{ref} = J_n(K_{pos} + K_{vel} \frac{d}{dt})(x^{rec} - x^{res})/2 + K_{for}(f^{rec} - \hat{f}^{rfob})/2 + \hat{f}^{dis}. \quad (6)$$

A block diagram of the motor control using MRS is shown in Fig. 1. In the Fig. 1, unlike a typical MRS, a noise signal is added to the force reference value, and a low-pass filter is applied to the feedback signal. These additions are necessary for the proposed method and were incorporated into MRS to standardize the experimental environment. The reasons for including these components are discussed in Sections II-C and II-D.

However, even with MRS, if the impedance of the motion and that of the environment differ, the motion data is not perfectly reproduced. As mentioned in Section I, this issue often leads to problems such as damage to the object or dropping it. While methods that record multiple sets of motion data and select the motion based on environmental information have been reported [21], they still need to be improved due to the finite number of motion data. These methods may only cover some scenarios or struggle with extrapolation, leaving unresolved issues.

C. PHYSICAL PROPERTY ESTIMATION

In this paper, motions are generated using environmental impedance. Since physical properties can represent environmental impedance, this section discusses methods for estimating these properties. Physical properties represent the relationship between position and force and are often described by the spring-mass-damper model. The mass M represents inertia, the damper D represents viscosity, and the spring K represents stiffness [22]. We have already proposed estimating physical properties using four parameters in the spring-mass-damper model with an added load H [23], [24]. The load primarily represents disturbances such as friction or ripple and components of work exerted on the contact object. Hence, the relationship between position X and force F is represented by (7).

$$F(s) = (Ms^2 + Ds + K)X(s) + H. \quad (7)$$

Each parameter was sequentially estimated using multiple regression analysis. The details of the algorithm are deferred to the references. The sampling time was 0.1 ms, and the most recent data of 100 ms was used, resulting in a sample size N of 1000.

When estimating physical properties, ensuring the signal's persistence of excitation (PE) is necessary. In other words, if the frequency components of the input signal are sparse, high-order model identification may not be correctly performed. Previous studies have applied a constant disturbance signal, but applying a large disturbance signal at the onset of contact can lead to improper contact due to vibrations [21]. Conversely, if the disturbance signal is too small, strong contact forces can suppress the disturbance signal, making it impossible to ensure PE. Therefore, an attempt was made to modulate the disturbance signal's amplitude based on the contact disturbance's magnitude. Equations (8) and (9) represent the amplitude $f_{\text{amp}}^{\text{noise}}$ and the disturbance signal f^{noise} .

$$f_{\text{amp}}^{\text{noise}} = \frac{1}{N} \int_0^N \hat{f}^{\text{dis}}(t) dt, \quad (8)$$

$$f^{\text{noise}} = f_{\text{amp}}^{\text{noise}} \{ \sin(2\pi 50t) + \sin(2\pi 60t) \\ + \sin(2\pi 70t) + \sin(2\pi 80t) \\ + \sin(2\pi 90t) + \sin(2\pi 100t) \}. \quad (9)$$

The method of imparting disturbance signals and the control system are described in Section II-D.

D. PROPOSED METHOD

This section details the proposed method. The method generates motions by estimating the environmental impedance of a new object based on two sets of motion data previously acquired. In this paper, the samples touched during the acquisition of the two sets of past motion data are referred to as Samples A and B, while the new sample is Sample C. Furthermore, the subscript numbers correspond to the sample numbers. The motion data for Sample C is assumed to be the

sum of the motion data for Samples A and B, each multiplied by a weight α_A and α_B . Consequently, the target values for position, velocity, acceleration, and force for Sample C are represented by (10)–(13).

$$x_C = \alpha_A x_A + \alpha_B x_B \quad (10)$$

$$\dot{x}_C = \alpha_A \dot{x}_A + \alpha_B \dot{x}_B \quad (11)$$

$$\ddot{x}_C = \alpha_A \ddot{x}_A + \alpha_B \ddot{x}_B \quad (12)$$

$$f_C = \alpha_A f_A + \alpha_B f_B. \quad (13)$$

It should be noted that the sum of the weights α_A and α_B is defined to be 1.

$$\alpha_A + \alpha_B = 1. \quad (14)$$

From (7), the relationship between the environmental impedance, position, and force in Sample C is represented in the time domain by (15).

$$f_C = m_C \ddot{x} + d_C \dot{x} + k_C x_C + H_C. \quad (15)$$

By substituting (10)–(13) into (15) and solving the simultaneous equations with (14), the values of α_A and α_B can be obtained from (16) and (17), and the denominator den of each is given by (18).

$$\alpha_A = \frac{H_C - f_B + k_C x_B + d_C \dot{x}_B + m_C \ddot{x}_B}{den} \quad (16)$$

$$\alpha_B = \frac{-(H_C - f_A + k_C x_A + d_C \dot{x}_A + m_C \ddot{x}_A)}{den} \quad (17)$$

$$den = f_A - f_B + k_C (x_B - x_A) \\ + d_C (\dot{x}_B - \dot{x}_A) + m_C (\ddot{x}_B - \ddot{x}_A). \quad (18)$$

The block diagram of the proposed method is shown in Fig. 2. The sequence of control actions for an unknown environment (Sample C) is as follows:

- Step 1** Acquire motion data using Samples A and B.
- Step 2** Sequentially determine the environmental impedance of Sample C as described in section II-C.
- Step 3** Calculate α from (16)–(18) based on the motion data of Samples A and B and the environmental impedance of Sample C.
- Step 4** Determine the command values for position and force using the calculated α_A and α_B by (10) and (13).
- Step 5** Perform control using the hybrid controller described in section II-A.

Note that Steps 2 to 5 are repeated for each sampling time. Additionally, if there is insufficient data to determine the environmental impedance in Step 2, i.e., if the number of samples is less than N , control is performed with $\alpha_A = 1$ and $\alpha_B = 0$. In addition, if the denominator den is sufficiently small, the value of α becomes indeterminate; therefore, if den is less than 0.001, control is also performed with $\alpha_A = 1$

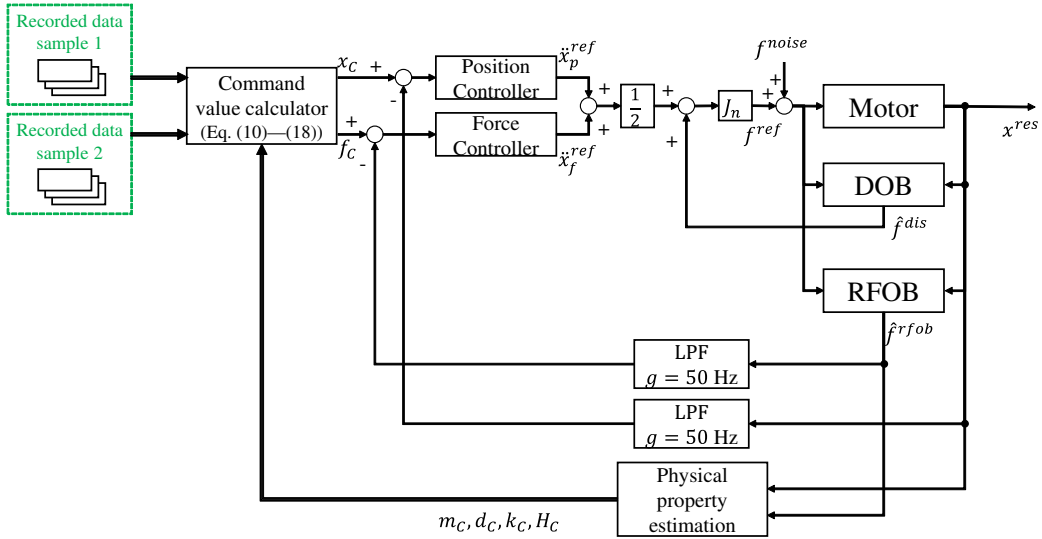


FIGURE 2: Block diagram with proposed method

and $\alpha_B = 0$. After determining the acceleration reference value in Step 5, as Section II-C outlines, the procedure involves introducing a noise signal to the reference. However, incorporating noise into the position and force readings can distort the impedance estimation. This complication arises because the interplay between input and output (position and force) extends beyond the direct path involving the motor and the gripped object to include the reciprocal path via the controller. To address this problem, our method employs a low-pass filter with a cutoff frequency of 50 Hz for the feedback of position and force values. Filtering out the noise enables the hybrid controller to produce an acceleration reference devoid of noise components, thereby facilitating precise impedance estimation for both the motor and the object.

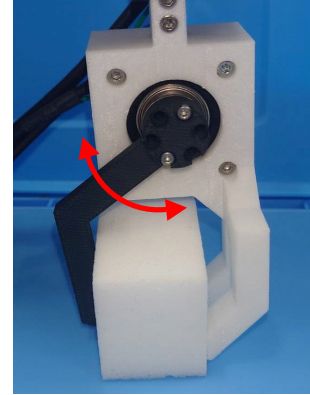


FIGURE 3: Device that performs grasping operation

III. EXPERIMENTAL METHODS

A. EXPERIMENTAL SETUP

This research developed an experimental apparatus capable of performing gripping actions with a single-degree-of-freedom rotary motor. This experimental setup can grip specific objects using a rotary motor, and the specific setup can be seen in the photograph shown in Fig. 3. The detailed specifications of the motor used are compiled in Table 1. The gripping mechanism adopted a cross-type hand shape [15]. Using the cross-type hand made it possible to grip soft materials without the fingers interfering with each other. In all experiments, the initial position was set to the moment the fingers touched the sample. The determination of whether the fingers had touched the sample was made visually.

B. SAMPLES

Eight types of samples with varied impedance characteristics were prepared for the experiments to represent common control challenges in adaptive impedance control and ensure diverse conditions for validation. The eight types of samples

TABLE 1: Motor specifications used in the experiment

Type	MDH-4018-6750EG03SH (manufactured by Microtech Laboratories, Inc.)
Moment of inertia J_n [kg · m ²]	0.000013589
Resolution	6750
Gear ratio	3.0
Proportional gain K_{pos} [1/s ²]	22500
Differential gain K_{vel} [1/s]	300
Force gain K_{for} [-]	1.0
Cutoff frequency of DOB [rad/s]	800

are as follows:

- Balloons
- Puffs
- Sponges
- Vinyl balls
- Soft springs
- Hard springs
- Erasers
- Wood blocks

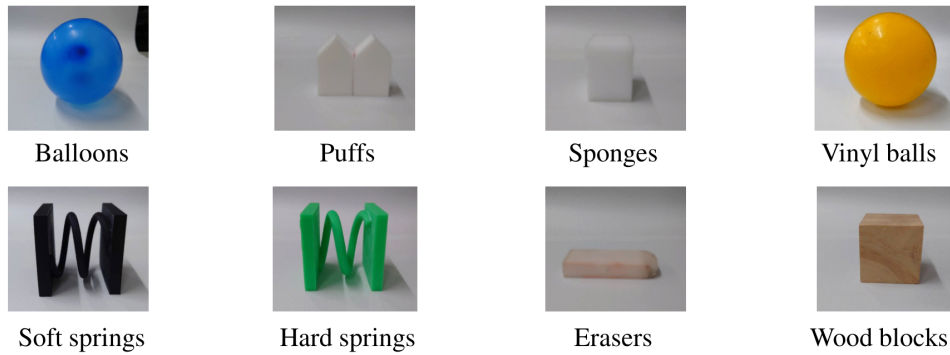


FIGURE 4: Eight samples used in the experiment

TABLE 2: The sample numbers for each sample are listed in each experiment. If a sample number is not mentioned, it was not used in that particular experiment. When pressed with a force of 0.2 Nm, the stiffness values are also provided.

Samaples	Balloons	Puffs	Sponges	Vinyl balls	Soft springs	Hard springs	Erasers	Wood blocks
Position control	1	2	3	4	5	6		
Force control	1		2	3		4	5	6
Stiffness [Nm/rad]	1.35	1.71	2.05	3.12	3.86	4.88	6.92	13.68

These samples were chosen to represent objects with different characteristics in the study of gripping actions. However, using too-hard samples can complicate control in position control experiments. As a result, distinct sets of six samples, chosen from eight, were utilized for the position and force control experiments to address this issue. Details of the eight types of samples are shown in photographs in Fig. 4, and Table 2 lists the samples used in each control experiment along with their corresponding sample numbers.

Additionally, impedance identification tests were conducted for each sample before the experiments. In these tests, the samples were gripped with a force of 0.2 Nm, and the impedance values at that time were measured. Based on the measured impedance, sample numbers were assigned in ascending order of the samples' stiffness.

C. CONTROL METHODS

This paper collected data for both position control and force control, and verification was performed based on the data reproduced in different samples. This section describes the data collected for each type of control.

In the position control experiments, the position command value was set as

$$x^{\text{cmd}} = \frac{\pi}{9}(-\cos(2\pi t/10) - \cos(2\pi t/2) + 2) \text{ [rad]}. \quad (19)$$

Position control was executed such that x^{cmd} in (2) became the position command value. The force command value was set as

$$f^{\text{cmd}} = 0.2(-\cos(2\pi t/10) - \cos(2\pi t/2) + 2) \text{ [Nm]}, \quad (20)$$

in the force control experiments. Force control was implemented so that f^{cmd} in (3) became the force command value.

In both cases, the command values were the superposition of two sine waves designed to maintain a gripping state.

D. VERIFICATION METHOD

In this paper, we first compared the accuracy of reproducing motion data through position control. Position control was performed on two selected samples (hereafter referred to as Sample A and B), and three types of control were applied to the remaining four samples: using the data from Sample A with MRS, the data from Sample B with MRS, and the data from both Sample A and B with the proposed method. Because of the results of position control on Samples A and B, the original position command values were used for comparison to ensure a fair evaluation. The root mean square error (RMSE) was then calculated based on the original position command values.

The two selected samples were tested in four combinations as follows:

- Pattern 1** Sample 1 and 6 (the two outermost samples)
- Pattern 2** Sample 3 and 4 (the two innermost samples)
- Pattern 3** Sample 1 and 2 (the two soft samples)
- Pattern 4** Sample 5 and 6 (the two hard samples)

Patterns 1 and 2 correspond to interpolation and extrapolation, respectively. Generally, machine learning methods exhibit unstable behavior for extrapolated actions that have yet to be learned. The proposed method generates actions without learning, and its effectiveness, even for extrapolation, was verified. In Patterns 3 and 4, we tested the capability to generate actions for samples with stiffness levels that differ from those of the samples used to collect the initial motion data.

Secondly, verification was conducted using force control, following the same sample selection as in the position control experiments. In this experiment, six samples, as shown in

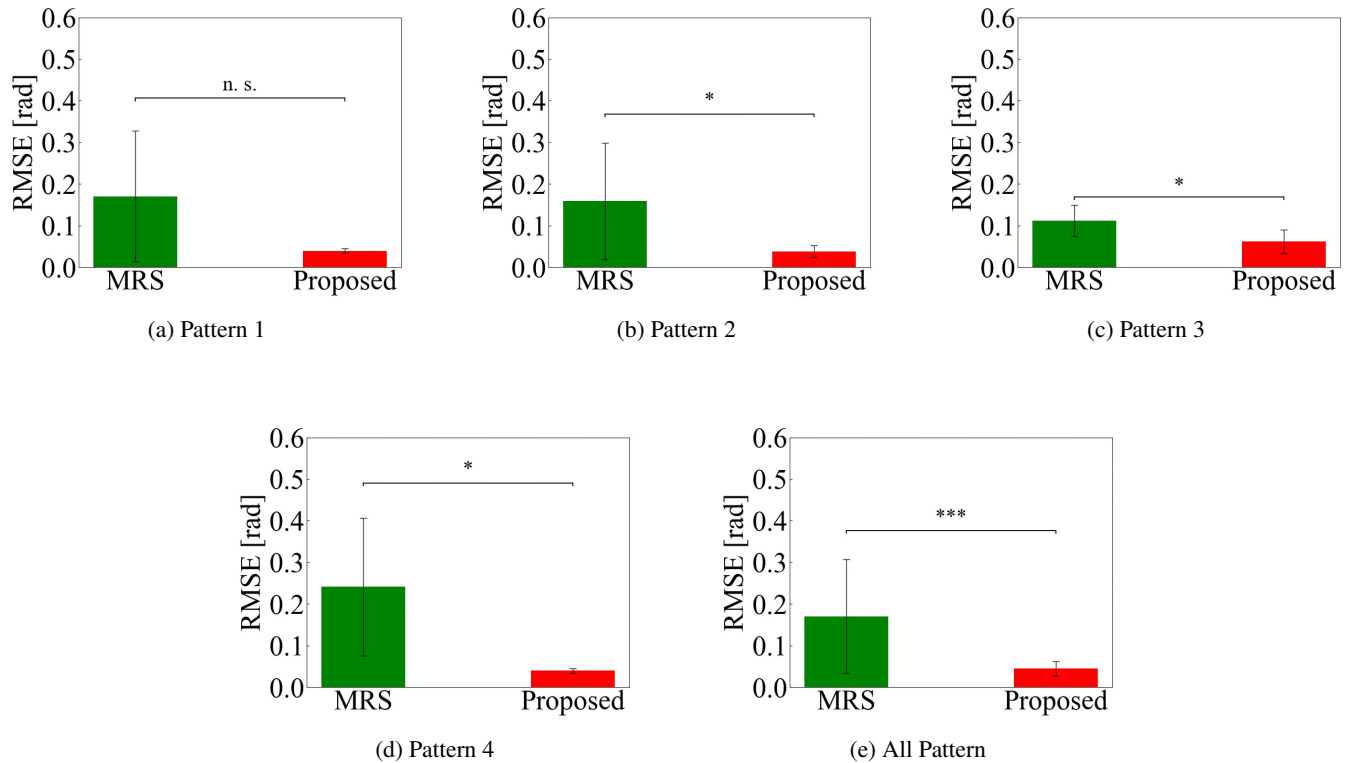


FIGURE 5: RMSE and t-test results based on position control recorded data. (* indicates $p < 0.05$, ** indicates $p < 0.01$, *** indicates $p < 0.001$, and n.s. means $p \geq 0.05$.)

Table 2, were used. Three types of control were executed, and the force response values were evaluated against the original force command values, namely (20), using RMSE.

IV. EXPERIMENTAL RESULTS

A. POSITION CONTROL

This section discusses the results of reproducing actions using position control. MRS was executed a total of 32 times, and the proposed method a total of 16 times, with neither resulting in any instances of control instability. Therefore, the success rate of the gripping action itself was 100%. These results confirmed that the proposed method retains the environmental adaptability possessed by MRS.

The RMSE for each pattern, utilizing both MRS and the proposed method, is depicted in Figs. 5(a)–(d), with the combined RMSE for all patterns shown in Fig. 5(e). The significance of these errors was assessed using the t-test, revealing a notable difference between MRS and the proposed method across all patterns except for Pattern 1. In Pattern 1, the standard deviation of the RMSE for MRS was larger compared to other patterns. Pattern 1 was the only pattern with a large difference in stiffness between the used samples. For example, employing Sample 2 was used as Sample C, MRS with Sample 1 led to smaller errors, whereas using Sample 6 resulted in greater errors. This indicated that the standard deviation of RMSE for MRS across the four samples increased. Given that the mean and standard

deviation of RMSE for the proposed method in Pattern 1 were not significantly different from those in other patterns, it suggests that the variability in MRS results was a key factor in the absence of a significant difference. The results shown in Fig. 5(e) show that the average RMSE for MRS was 0.170 rad, and the average RMSE for the proposed method was 0.0446 rad. Therefore, it was confirmed that the proposed method reduced errors by 74% compared to MRS.

B. FORCE CONTROL

Next, we present the outcomes of reproducing actions using force control data. Similar to the experiments with position control, no instances of motor runaway were observed in the force control trials. Consequently, the success rate of the gripping action reached 100%, confirming the proposed method’s ability to maintain the MRS adaptability to environmental changes even when utilizing force control data.

The RMSE for each pattern, employing both MRS and the proposed method, is depicted in Figs. 6(a)–(d). The aggregate RMSE across all patterns is presented in Fig. 6(e). A significant difference was noted between the performances of MRS and the proposed method across all patterns, with Pattern 1 showing the most pronounced difference. However, it’s important to acknowledge that a direct comparison is challenging due to the use of different samples for the position and force control experiments. The results shown in Fig. 6(e) show that the average RMSE for MRS was 0.0591

Nm, while the average RMSE for the proposed method was 0.0180 Nm. Therefore, it was confirmed that the proposed method reduces errors by 70% compared to MRS.

C. DISCUSSION

Through two verifications, it was confirmed that the proposed method significantly improves the reproducibility of actions compared to MRS. MRS attempts to reproduce motion data based on the relationship between position and force determined by the original target's impedance. In contrast, the proposed method recalculates position and force according to the current impedance, enhancing reproducibility. The rationale for this approach can be derived from the proposed method, as shown in (10)–(18). In the ideal case of position control, x_A , x_B , and x^{cmd} become equal. The same applies to velocity and acceleration. Consequently, according to (10)–(12) and (14), x_C becomes equal to x^{cmd} . Moreover, by defining $den = f_A - f_B$ and substituting $x_A = x_B = x^{\text{cmd}}$ into (16) and (17) and applying the result to (13) as:

$$f_C = m_C \ddot{x}^{\text{cmd}} + d_C \dot{x}^{\text{cmd}} + k_C x^{\text{cmd}} + H_C. \quad (21)$$

Equation (21) implies that if the motion data for Samples A and B were for position control, then the force command value f_C for Sample C is the force necessary to reach position x^{cmd} , given the environmental impedance m_C , d_C , k_C , H_C . Similarly, for force control, x_C becomes equal to the position required for exerting f_C against the current environmental impedance. Therefore, it has been verified that the proposed method generates actions adapted to the current target by matching the impedance of the two motion data sets with the environmental impedance.

Moreover, we confirmed the efficacy of the proposed method for samples with extrapolated impedance. Methods based on learning models usually interpolate the training data with approximations. Yet, beyond the scope of the training data, these methods might generate actions misaligned with user intentions in extrapolation scenarios. As described (21), the proposed method designs actions influenced by the current environmental impedance, thus facilitating adaptation to environments significantly divergent from the initial dataset. The uniform results demonstrate this adaptability for Patterns 2, 3, and 4, where extrapolation in both position and force control shows no notable variance from expected outcomes.

This method generates actions based on two sets of preliminary data. In contrast, conventional machine learning-based motion generation methods require at least several dozen pieces of training data. This difference demonstrates that our method offers significant design, implementation, and practical advantages compared to machine learning approaches. However, machine learning methods include learning rough action plans (for example, recognizing the position of an object and moving forward or to the right accordingly) in the learning process. In contrast, our method does not undertake the generation of this planning part of the action. Therefore, it necessitates the design of a simple action planner. An MRS that compensates for variations in the location of objects

based on image information has already been proposed [25], [26]. By integrating these, there is a potential to realize an MRS that adapts to objects' location and physical properties. Our method focuses on simplifying the action correction part, and its usefulness in this field remains significant.

Additionally, a significant advantage of the proposed method is its ability to generate actions without altering existing stable control systems. Traditional methods require adjustments to the control system, such as tuning the gains, making it essential to consider stability. However, our method assumes a stable control system, eliminating the need for additional discussions on stability. The only requirement for applying our method is the ability to measure and control position and force, making it easily applicable to existing manipulators and mobile units.

D. LIMITATION

This paper estimated the impedance of the grasped object using multiple regression analysis with a 0.1 s time window, as described in Section II-C. In the current experimental environment, where the motor continuously performs grasping actions, sudden changes in impedance were not observed. However, in actual use environments, the repetition of contact and non-contact is expected, which means that changes in impedance could occur within the time window. If the impedance changes within the time window, it could lead to a decrease in the accuracy of the estimation. Therefore, exploring new methods for effectively estimating impedance within shorter time windows is necessary.

In this study, we demonstrated the efficacy of our proposed method through experiments using a single-degree-of-freedom rotary motor. In addition, we evaluated tasks in two distinct patterns: position control and force control. Given that this research is a foundational study, verification under simplified conditions was deemed necessary. The achievement in tasks exhibiting extreme impedance patterns is predicated on the assumption that similar outcomes can be anticipated for tasks with intermediate impedance values. Future work will focus on verification efforts using manipulators with multiple degrees of freedom and action data featuring intermediate impedance levels.

V. CONCLUSION

In this paper, we proposed a new method to enhance the adaptability of robot actions under diverse environmental conditions by matching the impedance of actions and the environment. This method is based on obtaining the impedance of actions from two sets of prior motion data and sequentially estimating the environmental impedance based on position and force information. Experiments conducted under conditions of differing action impedances, namely position control (with infinite impedance) and force control (with zero impedance), confirmed that the proposed method can reproduce actions adapted to the current environment.

The proposed method's most significant advantage is its ability to generate effective actions with less data than ma-

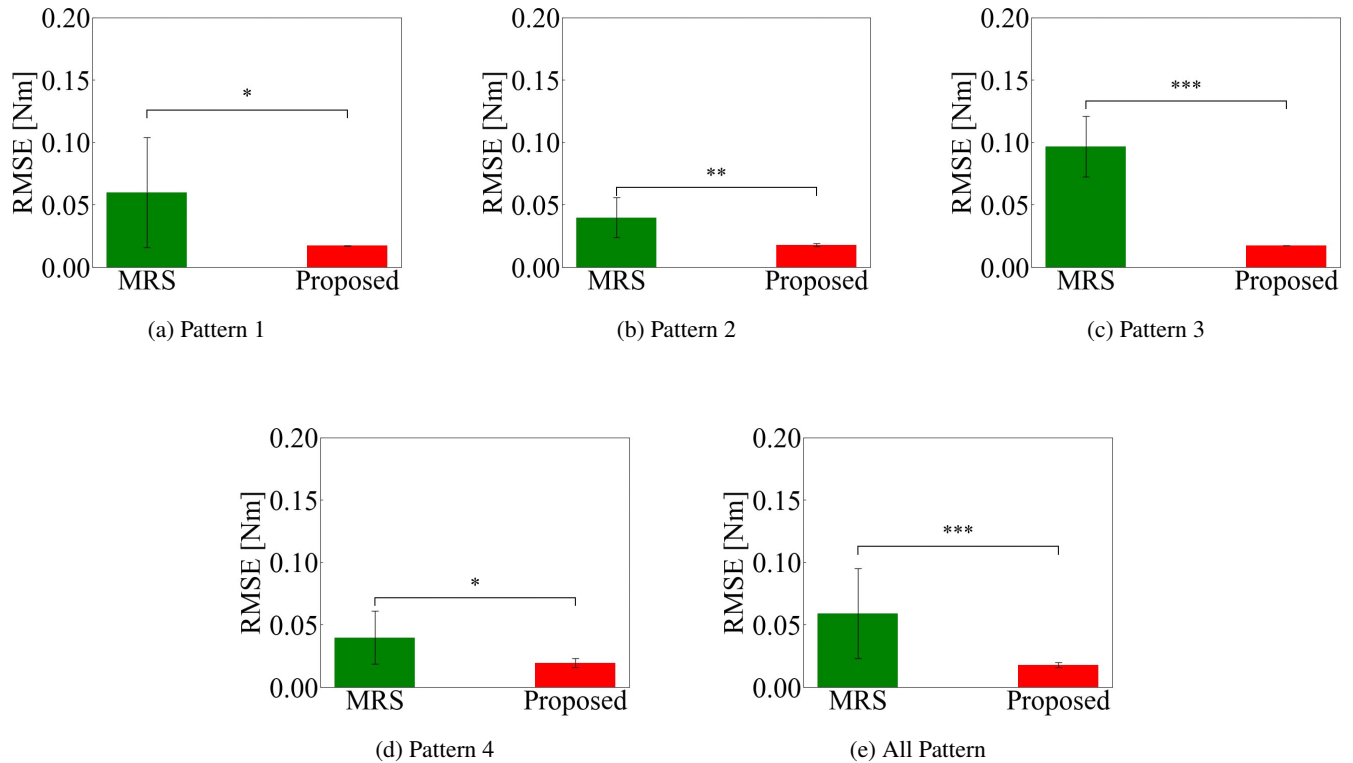


FIGURE 6: RMSE and t-test results based on force control recorded data. (* indicates $p < 0.05$, ** indicates $p < 0.01$, *** indicates $p < 0.001$, and n.s. means $p \geq 0.05$.)

chine learning-based methods. Additionally, it can be applied without changes to existing stable control systems, which is another significant benefit. These characteristics suggest that the proposed method has great potential in practical robot applications.

Future research will involve verification using motion data with intermediate impedance values. For example, this includes motion data where the impedance adjusts to grasp firmly when the object is rigid and gently when it is soft. Moreover, the focus will be on developing new estimation methods to effectively address changes in impedance in actions involving both contact and non-contact.

REFERENCES

- [1] L. Kunze, N. Hawes, T. Duckett, M. Hanheide, and T. Krajník: "Artificial Intelligence for Long-Term Robot Autonomy: A Survey," *IEEE Robotics and Automation Letters*, vol. 3, no. 4, pp. 4023–4030, 2018.
- [2] S. Bensalem, M. Gallien, F. Ingrand, I. Kahloul, and N. Thanh-Hung: "Designing Autonomous Robots," *IEEE Robotics and Automation Magazine*, vol. 16, no. 1, pp. 67–77, 2009.
- [3] D. Acemoglu and P. Restrepo: "Robots and Jobs: Evidence from US Labor Markets," *Journal of Political Economy*, vol. 128, no. 6, pp. 2188–2244, 2020.
- [4] E. Sariyildiz, G. Chen, and H. Yu: "An Acceleration-Based Robust Motion Controller Design for a Novel Series Elastic Actuator," *IEEE Transactions on Industrial Electronics*, vol. 63, no. 3, pp. 1900–1910, 2015.
- [5] T. Nozaki, T. Mizoguchi, and K. Ohnishi: "Decoupling Strategy for Position and Force Control Based on Modal Space Disturbance Observer," *IEEE Transactions on Industrial Electronics*, vol. 61, no. 2, pp. 1022–1032, 2013.
- [6] Y. Yokokura, S. Katsura, and K. Ohishi: "Stability Analysis and Experimental Validation of a Motion-Copying System," *IEEE Transactions on Industrial Electronics*, vol. 56, no. 10, pp. 3906–3913, 2009.
- [7] H. Tanaka and K. Ohnishi: "Haptic Data Compression/Decompression Using DCT for Motion Copy System," in *Proc. of IEEE International Conference on Mechatronics*, pp. 1–6, 2009.
- [8] Y. Nagatsu and S. Katsura: "Design Strategies for Motion Reproduction Based on Environmental Disturbance Compensation," *IEEE Transactions on Industrial Electronics*, vol. 62, no. 9, pp. 5786–5798, 2015.
- [9] K. Miura, A. Matsui, and S. Katsura: "Synthesis of Motion-Reproduction Systems Based on Motion-Copying System Considering Control Stiffness," *IEEE/ASME Transactions On Mechatronics*, vol. 21, no. 2, pp. 1015–1023, 2015.
- [10] M. Oikawa, T. Kusakabe, K. Kutsuzawa, S. Sakaino, and T. Tsuji: "Reinforcement Learning for Robotic Assembly Using Non-Diagonal Stiffness Matrix," *IEEE Robotics and Automation Letters*, vol. 6, no. 2, pp. 2737–2744, 2021.
- [11] T. Hachimine, J. Morimoto, and T. Matsubara: "Learning to Shape by Grinding: Cutting-surface-aware Model-based Reinforcement Learning," *IEEE Robotics and Automation Letters*, vol. 8, no. 10, pp. 6255–6262.
- [12] A. Lobbezoo, Y. Qian, and H. J. Kwon: "Reinforcement Learning for Pick and Place Operations in Robotics: A Survey," *Robotics*, vol. 10, 105, 2021.
- [13] T. Inoue, G. De Magistris, A. Munawar, T. Yokoya, and R. Tachibana: "Deep Reinforcement Learning for High Precision Assembly Tasks," in *Proc. of IEEE/RSJ International Conference on Intelligent Robots and Systems (IROS)*, pp. 819–825, 2017.
- [14] A. Sasagawa, S. Sakaino, and T. Tsuji: "Motion Generation using Bilateral Control-based Imitation Learning with Autoregressive Learning," *IEEE Access*, vol. 9, pp. 20508–20520, 2021.
- [15] K. Yamane, Y. Saigusa, S. Sakaino, and T. Tsuji: "Soft and Rigid Object Grasping with Cross-Structure Hand Using Bilateral Control-Based Imitation Learning," *IEEE Robotics and Automation Letters*, 2023.
- [16] B. Fang, S. Jia, D. Guo, M. Xu, S. Wen, and F. Sun: "Survey of Imitation Learning for Robotic Manipulation," *International Journal of Intelligent Robotics and Applications*, vol. 3, pp. 362–369, 2019.
- [17] D. K. Jha, S. Jain, D. Romeres, W. Yerazunis, and D. Nikovski: "Generalizable Human-Robot Collaborative Assembly Using Imitation Learning and

Force Control,” in *Proc. of European Control Conference (ECC)*, pp. 1–8, 2023.

- [18] T. Murakami, F. Yu, and K. Ohnishi: “Torque Sensorless Control in Multidegree-of-freedom Manipulator,” *IEEE Transactions on Industrial Electronics*, vol. 40, no. 2, pp. 259–265, 1993.
- [19] W. Iida and K. Ohnishi, “Reproducibility and operability in bilateral teleoperation,” in *Proc. of IEEE International Workshop on Advanced Motion Control (AMC)*, pp. 217–222, 2004.
- [20] S. Sakaino, T. Sato, and K. Ohnishi, “Multi-dof micro-macro bilateral controller using oblique coordinate control,” *IEEE Transaction on Industrial Electronics*, vol. 7, pp. 446–454, 2011.
- [21] T. Kitamura, X. Sun, Y. Saito, H. Asai, T. Nozaki, and K. Ohnishi: “Motion Generation Based on Physical Property Estimation in Motion Copy System,” in *Proc. of International Workshop on Advanced Motion Control (AMC)*, pp. 62–67, 2022.
- [22] M. Nagurka and S. Huang: “A Mass-Spring-Damper Model of a Bouncing Ball,” in *Proc. of the American Control Conference*, vol. 1, pp. 499–504, 2004.
- [23] T. Kitamura, A. Saito, K. Yamazaki, Y. Saito, H. Asai, and K. Ohnishi: “Validation of a Property Estimation Method Based on Sequential and Posteriori Estimation,” in *Proc. of Annual Conference of the IEEE Industrial Electronics Society (IECON)*, 2022.
- [24] K. Ohnishi and Y. Saito: “Quantification of Force/Tactile Sensation,” *IEEE Journal of Industry Applications*, vol. 12, no. 2, pp. 125–130, 2023.
- [25] T. Nozaki, T. Mizoguchi, and K. Ohnishi: “Motion Reproduction Using Time-Scaling for Adaptation to Difference in Environmental Location,” in *Proc. of IEEE International Conference on Industrial Technology (ICIT)*, pp. 45–50, 2014.
- [26] X. Sun, T. Nozaki, T. Murakami, and K. Ohnishi: “A Method to Make a Robot Understand What Was a Target Object in Motion Copying System,” in *Proc. of IEEE International Workshop on Advanced Motion Control (AMC)*, pp. 241–246, 2020.



HIROSHI ASAI received the B.E., M.E., and Ph.D. degrees in electrical and computer engineering from Yokohama National University, Japan, in 2014, 2016, and 2019 respectively. Since 2019, he has been with Haptics research center in Keio University, Kanagawa, where he is currently an Project Assistant Professor. His research interests include linear permanent magnet machines and motion control.



TOMOYA KITAMURA received the B.E., M.E., and Ph.D degrees in electrical and electronic systems engineering from Saitama University, Saitama, Japan, in 2015, 2017, and 2021, respectively. From 2021 to 2024, he was a Project Assistant Professor with Keio University, Kawasaki, Japan. Since 2024, he has been an Assistant Professor with Tokyo University of Science, Noda, Japan. His research interests include mechatronics, haptics, and biomedical engineering.



KOUHEI OHNISHI received Ph.D. in electrical engineering from the University of Tokyo in 1980 and has been with Keio University since then. He received IEEE Outstanding Achievement Award in 2008 and IEEE Meritorious Contribution Award in 2017. His research field includes motion control, haptics, power electronics, and robotics.

...



YUKI SAITO received the B.E. degree in system design engineering and the M.E., and Ph.D. degrees in integrated design engineering from Keio University, in 2011, 2013 and 2018, respectively. He has been with Keio University since 2018, where he is currently a Project Assistant Professor. His research interests include motion control, electronics, and haptics.